Quantitative Magnetization Transfer Imaging at 7 Tesla: Application in Multiple Sclerosis Patients and Validation in Postmortem Brain

Richard D. Dortch[1,2], Adrienne N. Dula[1,2], Francesca Bagnato[1,2], David R. Pennell[1,2], Siddharama Pawate[3], Simon Hametner[4], Hans Lassmann[4], John C. Gore[1,2], and Seth A. Smith[1,2]

[1]Radiology and Radiological Sciences, Vanderbilt University, Nashville, TN, United States, [2]Vanderbilt University Institute of Imaging Science, Vanderbilt University, Nashville, TN, United States, [3]Neurology, Vanderbilt University, Nashville, TN, United States, [4]Center for Brain Research, Medical University, Vienna, Austria

Target Audience: 1) imaging scientists interested in quantitative imaging at high field and 2) the White Matter Study Group of the ISMRM

Purpose: Quantitative magnetization transfer (qMT) imaging has been previously used to assay myelin content in white matter [1–4]. Although promising, qMT imaging is often limited by long scan times. To decrease scan times, we recently [5] developed a selective inversion recovery (SIR) qMT protocol that exploits the increased signal-to-noise ratio (SNR) available at 7.0 T. Similar to previous work at lower fields [1–4], results from this high-field study suggest that macromolecular to free pool-size-ratio (*PSR*) is related to myelin content in healthy controls. The goals of the study herein are: 1) to establish the relationship between *PSR* and pathological changes in relapsing-remitting multiple sclerosis (RRMS) patients and 2) to validate the SIR technique by comparing qMT parameter maps in *postmortem* RRMS brains to histological measurements of myelin content.

Methods: Postmortem Sample Processing: Three samples were donated from the Rocky Mountain MS brain bank (Englewood, Colorado). Samples were fixed (10% formalin), sectioned into 10-mm coronal slices, placed in an MR-compatible holder filled with fixative, and MRI was performed. Following MRI, the sample was dehydrated and embedded, sectioned into 3-5 μm slices, stained for myelin using Luxol fast blue (LFB), and light microscopy was performed. Data Acquisition: SIR data were collected in five healthy volunteers (23–38 y.o.), six RRMS patients (33–65 y.o.), and three *postmortem* brains using a 7.0-T Philips MR scanner with a 32-channel head receive coil. The pulse sequence [5] employed a B_0- and B_1^+-insensitive inversion pulse, a variable duration inversion recovery period to sample the MT-related biexponential recovery, and a turbo field echo (TFE) readout. Data were acquired in *postmortem* brains using: inversion times = 6–2000 ms (16 values), predelay time = 1.0 s, TFE pulse interval/TE/flip angle = 5.6 ms/2.6 ms/15°, echoes per shot = 71, resolution = $0.7{\times}0.7{\times}0.7$ mm^3, and field-of-view (FOV) = $150{\times}150{\times}28$ mm^3. A similar, lower resolution ($2{\times}2{\times}3$ mm^3, FOV = $212{\times}212{\times}75$ mm^3), protocol was used for *in vivo* studies (see [5] for details). Data Analysis: SIR-TFE data were fit to a biexponential model of the MT effect and the resulting rate constants and amplitudes were related to qMT parameters [6], including: *PSR*, the MT rate from the free to macromolecular pool (k_{mf}), and the R_1 of the free pool (R_{1f}). For the *in vivo* studies, normal-appearing white matter (NAWM) was segmented by thresholding the R_{1f} maps and a histogram analysis was performed. For each histogram, the parameter value at the maximum histogram value (P_m) and the root-mean-squared deviation about P_m (RMSD) were tabulated. For the *postmortem* studies, ROIs were defined in lesions, NAWM, and normal-appearing gray matter (NAGM) in the qMT parameter maps and corresponding histology slides. Pearson's correlation coefficient was tabulated to assess the relationship between qMT parameters and the optical density (OD) of the LFB sections.

Results and Discussion: *In vivo* studies: Fig. 1 shows sample parameter maps from a healthy volunteer (top tow) and RRMS patient (middle row) along with corresponding histograms from NAWM (bottom row). Focal decreases in *PSR* and R_{1f} were observed in lesions (black arrow). In addition, shifted and broadened parameter histograms were observed for *PSR* (healthy: P_m = 17±1%, RMSD = 2±1%; RRMS: P_m = 15±2%, RMSD = 3±1%) and R_{1f} (healthy: P_m = 0.65±0.03 s^{-1}, RMSD = 0.07±0.02 s^{-1}; RRMS: P_m = 0.60±0.08 s^{-1}, RMSD = 0.08±0.04 s^{-1}) throughout NAWM. Consistent with a previous study of spinal WM [7], similar k_{mf} values were observed in healthy and RRMS brains. While these results suggest that *PSR* and R_{1f} are sensitive to changes in myelin content, other pathological features (e.g., inflammation, axonal loss) may also be contributing to the observed differences between the healthy and RRMS cohorts. The *postmortem* study was designed to assess the relationship between myelin content and the SIR-derived parameters. *Postmortem* studies: Fig. 2 (top row) shows a sample LFB section and corresponding qMT parameter maps. Similar to the *in vivo* results, focal decreases were observed in *PSR* and R_{1f} within lesions (black arrows) in the *postmortem* brains. From the correlation analysis (bottom row), a significant correlation between *PSR* and myelin content was detected. Note the increase in *PSR* relative to the *in vivo* studies, which is likely due to cross-linking from fixation. R_{1f} correlated more strongly with myelin content than *PSR*; however, this stronger correlation is likely driven by the lower uncertainty in the R_{1f} estimate [6] and may be nonlinear (see dashed gray line) due to the sensitivity of R_{1f} to other pathological features (e.g., inflammation). Consistent with the *in vivo* findings, a weak correlation was detected between k_{mf} and myelin content (r^2 = 0.24, p = 0.04). Together, these results suggest that *PSR* (and potentially R_{1f}) values can be used as a marker for myelin content in RRMS patients at 7.0 T.

References: [1] Sled. *MRM* **46**: 923 (2001). [2] Yarnykh. *Neuroimage* **23**: 409 (2004). [3] Garcia. *Neuroimage* **52:** 532 (2010). [4] Undehill. *Neuroimage* **47:** 1568 (2009). [5] Dortch. *Neuroimage* **64**:640 (2012). [6] Li. *MRM* **64**: 491 (2010). [7] Smith. *MRM* **61**: 22 (2009).
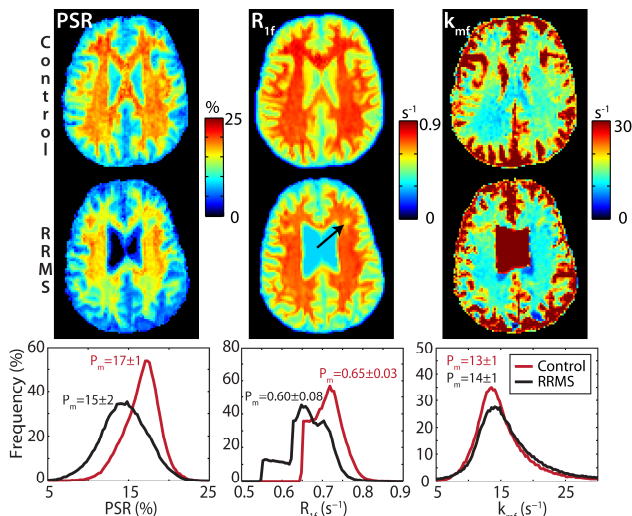
Fig. 1. Parameter maps from a control (top) and RRMS patient (middle) and mean NAWM histograms across each cohort (bottom).
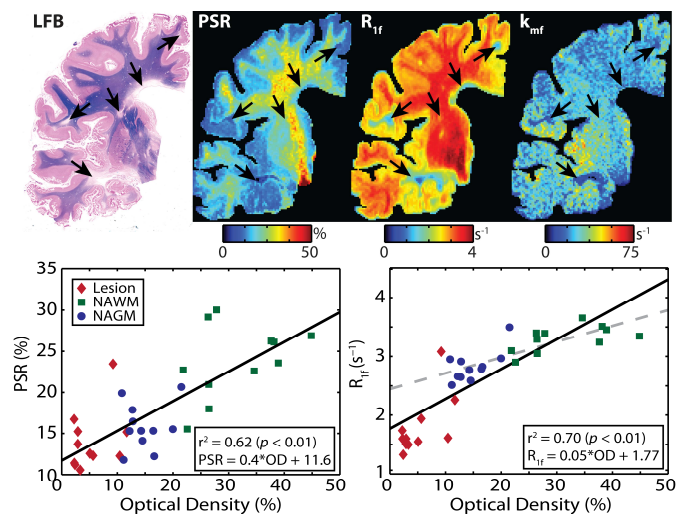

Fig. 2. *Postmortem* histology and SIR parameter maps from a representative brain (top) and scatterplot of *PSR* and R_{1f} versus the LFB-derived OD values (bottom).